



Contents lists available at ScienceDirect

Biochemical and Biophysical Research Communications

journal homepage: www.elsevier.com/locate/ybbrc

The heterozygous R155C VCP mutation: Toxic in humans! Harmless in mice?

Christoph S. Clemen^{a,b,*}, Lilli Winter^{c,d}, Karl-Heinz Strucksberg^b, Carolin Berwanger^{a,b}, Matthias Türk^e, Cornelia Kornblum^{f,g}, Alexandra Florin^h, Juan Antonio Aguilar-Pimentelⁱ, Oana Veronica Amarie^{i,j}, Lore Beckerⁱ, Lillian Garrett^{i,j}, Wolfgang Hansⁱ, Kristin Morethⁱ, Frauke Neff^{i,k}, Laura Pinggenⁱ, Birgit Rathkolb^{i,l,m}, Ildikó Rácz^{n,o}, Jan Rozman^{i,m}, Irina Treiseⁱ, Helmut Fuchsⁱ, Valerie Gailus-Durnerⁱ, Martin Hrabe de Angelis^{i,m,p}, Matthias Vorgerd^a, Ludwig Eichinger^b, Rolf Schröder^{c,**}

^a Department of Neurology, Heimer Institute for Muscle Research, University Hospital Bergmannsheil, Ruhr-University Bochum, 44789, Bochum, Germany

^b Center for Biochemistry, Institute of Biochemistry I, Medical Faculty, University of Cologne, 50931, Cologne, Germany

^c Institute of Neuropathology, University Hospital Erlangen, Friedrich-Alexander University Erlangen-Nuremberg, 91054, Erlangen, Germany

^d Neuromuscular Research Department, Center for Anatomy and Cell Biology, Medical University of Vienna, 1090, Vienna, Austria

^e Department of Neurology, University Hospital Erlangen, Friedrich-Alexander University Erlangen-Nuremberg, 91054, Erlangen, Germany

^f Department of Neurology, University Hospital Bonn, 53125, Bonn, Germany

^g Center for Rare Diseases Bonn, University Hospital Bonn, 53127, Bonn, Germany

^h Institute for Pathology, University Hospital Cologne, 50937, Cologne, Germany

ⁱ German Mouse Clinic, Institute of Experimental Genetics, Helmholtz Zentrum München, German Research Center for Environmental Health, 85764, Neuherberg, Germany

^j Institute of Developmental Genetics, Helmholtz Zentrum München, German Research Center for Environmental Health, 85764, Neuherberg, Germany

^k Institute of Pathology, Helmholtz Zentrum München, German Research Center for Environmental Health, 85764, Neuherberg, Germany

^l Institute of Molecular Animal Breeding and Biotechnology, Gene Center, Ludwig-Maximilians-University München, 81377, Munich, Germany

^m German Center for Diabetes Research (DZD), 85764, Neuherberg, Germany

ⁿ Institute of Molecular Psychiatry, Medical Faculty, University of Bonn, 53127, Bonn, Germany

^o Clinic of Neurodegenerative Diseases and Gerontopsychiatry, University of Bonn Medical Center, 53127, Bonn, Germany

^p Chair of Experimental Genetics, School of Life Science Weihenstephan, Technische Universität München, 85354, Freising, Germany

ARTICLE INFO

Article history:

Received 30 July 2018

Accepted 4 August 2018

Available online 9 August 2018

Keywords:

VCP

p97

R155C VCP knock-in mice

IBMPFD

ALS

Multisystem proteinopathy

ABSTRACT

Heterozygous missense mutations in the human VCP gene cause inclusion body myopathy associated with Paget disease of bone and fronto-temporal dementia (IBMPFD) and amyotrophic lateral sclerosis (ALS). The exact molecular mechanisms by which VCP mutations cause disease manifestation in different tissues are incompletely understood. In the present study, we report the comprehensive analysis of a newly generated R155C VCP knock-in mouse model, which expresses the ortholog of the second most frequently occurring human pathogenic VCP mutation. Heterozygous R155C VCP knock-in mice showed decreased plasma lactate, serum albumin and total protein concentrations, platelet numbers, and liver to body weight ratios, and increased oxygen consumption and CD8⁺/Ly6C⁺ T-cell fractions, but none of the typical human IBMPFD or ALS pathologies. Breeding of heterozygous mice did not yield in the generation of homozygous R155C VCP knock-in animals. Immunoblotting showed identical total VCP protein levels in human IBMPFD and murine R155C VCP knock-in tissues as compared to wild-type controls. However, while in human IBMPFD skeletal muscle tissue 70% of the total VCP mRNA was derived from the mutant allele, in R155C VCP knock-in mice only 5% and 7% mutant mRNA were detected in skeletal muscle and brain tissue, respectively. The lack of any obvious IBMPFD or ALS pathology could thus be a consequence of the very low expression of mutant VCP. We conclude that the increased and decreased fractions of the R155C mutant VCP mRNA in man and mice, respectively, are due to missense mutation-induced, divergent alterations in the biological half-life of the human and murine mutant mRNAs. Furthermore,

* Corresponding author. Department of Neurology, Heimer Institute for Muscle Research, University Hospital Bergmannsheil, Ruhr-University Bochum, Bürkle-de-la-Camp-Platz 1, 44789, Bochum, Germany.

** Corresponding author. Institute of Neuropathology, University Hospital Erlangen, Schwabachanlage 6, 91054, Erlangen, Germany.

E-mail addresses: christoph.clemen@rub.de (C.S. Clemen), rolf.schroeder@uk-erlangen.de (R. Schröder).

our work suggests that therapy approaches lowering the expression of the mutant VCP mRNA below a critical threshold may ameliorate the intrinsic disease pathology.

© 2018 The Authors. Published by Elsevier Inc. This is an open access article under the CC BY-NC-ND license (<http://creativecommons.org/licenses/by-nc-nd/4.0/>).

1. Introduction

Missense mutations in the human VCP gene on chromosome 9p13-p12, which encodes an essential and evolutionarily highly conserved Triple-A ATPase (ATPase Associated with diverse cellular Activities) [1,2], cause various autosomal-dominantly inherited human diseases. Inclusion body myopathy (IBM) associated with Paget disease of the bone (PDB) and frontotemporal dementia (FTD), or IBMPFD (OMIM 605382), a late-onset multisystem disorder, was the first identified disease entity [3,4], followed by amyotrophic lateral sclerosis (ALS14) [5], Parkinson's disease (PD) [6,7], hereditary spastic paraplegia (HSP) [8,9], and Charcot-Marie-Tooth disease type 2 (HMSN2) [10]. Since the first description of pathogenic VCP mutations in 2004, over 40 different disease-causing missense mutations have been described [11].

The Mg^{2+} -dependent VCP protein exhibits a tripartite structure composed of an N-terminal CDC48 domain and the D1 and D2 domains that bind and hydrolyse ATP [12,13] (Fig. 1A). VCP monomers assemble into a ring-shaped hexamer with the D-domains forming a central cylinder surrounded by the CDC48 domains [14,15]. The multiple functions and the versatile cofactor binding of the VCP protein are essentially dependent on the energy derived from ATP hydrolysis [16]. VCP is centrally involved in multiple and diverse cellular processes such as membrane dynamics, protein quality control, cell cycle, apoptosis, and DNA damage response [17,18]. Moreover, recent work reported on mutation-specific effects on VCP interaction partners leading to alterations in the ratio of VCP monomers to hexamers [19] as well as functional consequences on endocytosis [20], endoplasmic reticulum associated degradation (ERAD) of proteins [21], ATPase activity [19], and 20S proteasome binding [22]. However, the exact molecular mechanisms leading from a VCP point mutation to specific disease manifestations affecting nervous, bone, and striated muscle tissues are currently unknown.

In the present study, we generated and characterized a R155C VCP knock-in mouse model expressing the ortholog of the human R155C VCP mutation, which has been shown to cause both IBMPFD [3,4] and ALS [5]. Though the failure to generate mice homozygous for the R155C VCP missense mutation clearly denotes a toxic effect not compatible with life, our comprehensive analyses of heterozygous mice resulted in multiple aberrant parameters, but did not reveal any VCP-typical pathology, as previously described in a R155H VCP knock-in mouse model [23]. The here presented findings are discussed in the context of the human and murine codon 155-related VCP pathologies.

2. Materials and methods

2.1. Animals

In the present study, we used heterozygous R155C (c.463_465delCGG>insTGT) VCP knock-in mice (B6J.B6-Vcp^{tm2.1Ccrs}) and their wild-type siblings. The mouse model was generated according to our specifications (CSC, RS) by genOway, Lyon, France. Routine genotyping was performed by PCR (primer pair 51546cre 5'-CAGTTCTCATGCTCTCTGAAGGATAATGT-3' and 51547cre 5'-TCTACAACCTTGAACCTCACAGCACGC-3'). In addition,

individual mice were genotyped by Southern blotting, and the presence of the R155C VCP point mutation was verified by sequencing; for details see Fig. 1B–E. Mice were housed in isolated ventilated cages (IVC) under specific and opportunistic pathogen-free (SOPF) conditions at a standard environment with free access to water and food. Health monitoring was done as recommended by the Federation of European Laboratory Animal Science Associations (FELASA). Mice were handled in accordance with the German Animal Welfare Act (Tierschutzgesetz) as well as the German Regulation for the protection of animals used for experimental purposes or other scientific purposes (Tierschutz-Verordnung). All investigations were approved by the governmental office for animal care (Landesamt für Natur, Umwelt und Verbraucherschutz North Rhine-Westphalia (LANUV NRW), Recklinghausen, Germany (reference numbers 8.87–50.10.47.09.014 and 84–02.05.40.14.057)).

2.2. Phenotypic analysis in the German Mouse Clinic

Heterozygous R155C VCP knock-in mice and wild-type control littermates were subjected to a systematic, comprehensive phenotyping screen at the German Mouse Clinic at the Helmholtz Zentrum München (<http://www.mouseclinic.de>) as described previously [24–27]. This screen covers a broad range of parameters in the areas of allergy, behavior, cardiovascular function, clinical chemistry, dysmorphology, energy metabolism, eye analysis and vision, hematology, immunology, neurology, and pathology. For further details see legend to Fig. 3.

2.3. Analysis of skeletal muscle tissue sections

Dissected murine skeletal muscle specimens were immediately frozen in liquid nitrogen-cooled isopentane. A human tissue sample was derived from a diagnostic skeletal muscle biopsy of a previously reported patient with a heterozygous R155C VCP mutation [28]. Cryostat sections of 6 μ m thickness were placed on microscope slides, air-dried for 30 min, stained using routine histochemistry protocols [29], and images were captured using an Olympus CX41 light microscope (Olympus, Hamburg, Germany). Ultrathin sections for transmission electron microscopy were prepared as described in Ref. [30] and examined with a Zeiss LEO 900 electron microscope (Carl Zeiss GmbH, Oberkochen, Germany).

2.4. Analysis of skeletal muscle tissue lysates and antibodies

For SDS-PAGE snap frozen samples of dissected muscles were ground, solubilized, and homogenized essentially according to [31–33]. The trypsin-like proteasomal activity of soleus muscles was determined as described in detail in Ref. [34]. Primary antibodies for immunoblotting were: VCP, mouse monoclonal antibody, 1:2000 in PBS-T with 5% milk powder, #11433, Abcam; strumpellin, rabbit polyclonal antibody, 1:500 in PBS-T, #sc-87445, Santa Cruz; sequestosome-1/p62, rabbit polyclonal antibody, 1:3000 in PBS-T, #P0067, Sigma Aldrich; BAG-3, rabbit polyclonal antibody, 1:3000 in PBS-T, #10599-1-AP, Proteintech; TDP-43 rabbit polyclonal antibody, 1:1000 in PBS-T, #12892-1-AP, Proteintech; ULK1, rabbit polyclonal antibody, 1:1000 in PBS-T, #ab65056,

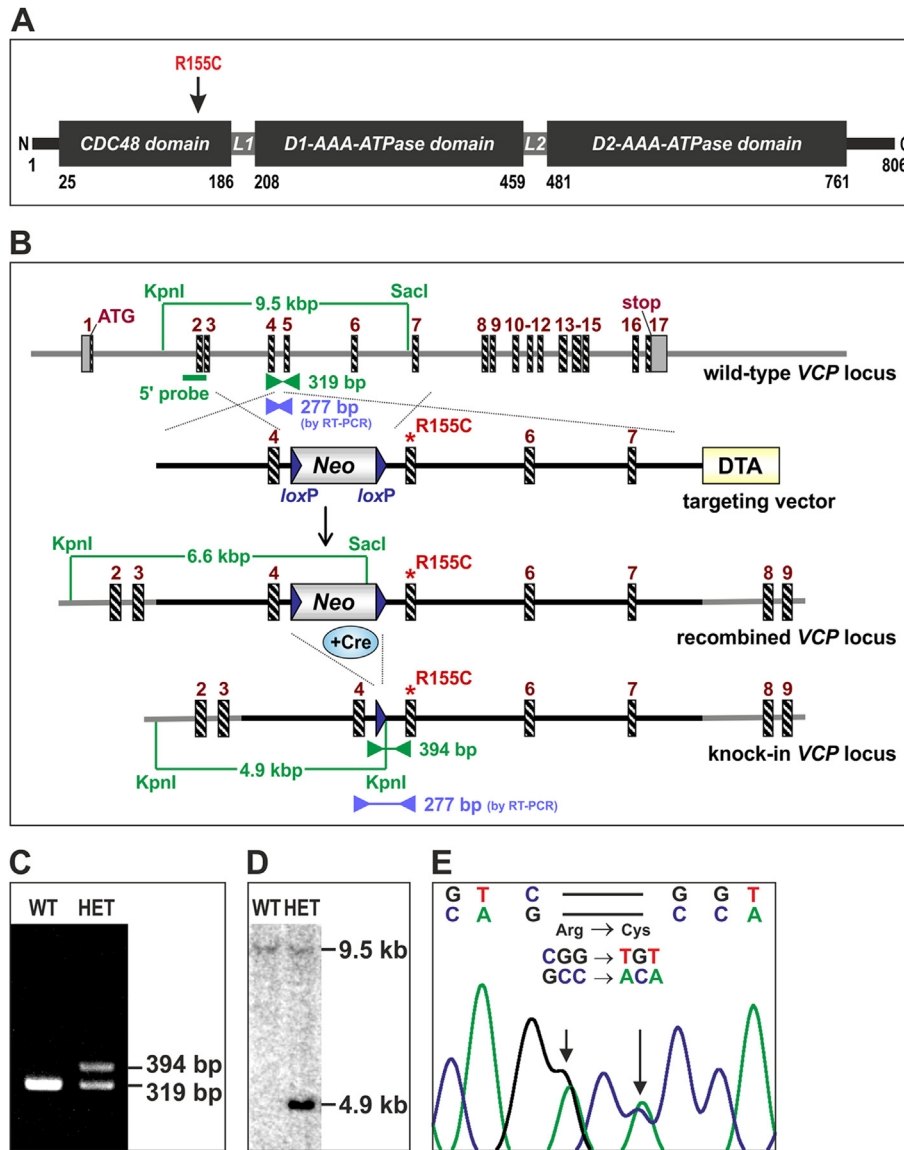


Fig. 1. Domain organization of the VCP protein and VCP gene targeting strategy. **A**, The murine and human VCP proteins are 100% identical on the amino acid level. The N-terminal region of the VCP protein harbors the CDC48 domain, in which the pathogenic R155C missense mutation is located, followed by the D1 and D2 ATPase domains and the C-terminal extension. **B**, Scheme of the genomic targeting strategy resulting in the R155C VCP knock-in mouse strain. **C**, PCR genotyping (green primer pair in (B)) confirms the presence of a knock-in allele with a 394 bp product containing the remaining single loxP site vs. 319 bp derived from the wild-type allele. **D**, Southern blot verification of the R155C VCP knock-in mice based on KpnI/SacI double-restriction digestion and hybridization with an external 5' probe leading to the detection of the expected 4.9 kb knock-in and 9.5 kb wild-type fragments. **E**, verification of the presence of the TGT missense mutation at the mRNA level encoding R155C VCP by sequencing of the indicated 277 bp RT-PCR product from heterozygous mice (blue primer pair in (B)), mVCPki3F 5'-AGCCATGCCCTGATGTTAAAG-3' and mVCPki3R 5'-TCCTCATCCTCTCGCTTGAT-3'. The chromatogram shows the expected double signal for CGG (Arg) and TGT (Cys) from the wild-type and knock-in alleles, respectively. (For interpretation of the references to colour in this figure legend, the reader is referred to the Web version of this article.)

Abcam; Beclin-1, rabbit monoclonal antibody, 1:500 in PBS-T, #3495, Cell Signaling.

2.5. VCP mRNA analysis

Complementary DNA derived from skeletal muscle of the above IBMPFD patient as well as skeletal muscle and brain tissue of heterozygous R155C VCP knock-in mice was used for PCR (human primer pair, hVCPki1F 5'-AATAACCTTCGTGTACGCCT-3', hVCPki3R 5'-TCCTCATCCTCTCGCTTGAT-3', product size 317 bp; murine primer pair, mVCPki3F 5'-AGCCATGCCCTGATGTTAAAG-3', mVCPki3R 5'-TCCTCATCCTCTCGCTTGAT-3', product size 277 bp). To analyze the ratio of wild-type and mutant VCP mRNA, PCR

products were directly subjected to restriction digestion as well as cloned into pGEM-Teasy (Promega Corporation, Madison, WI, USA) and transformed into *E. coli*. Single colonies were picked, used for a second PCR, and the obtained PCR products also were subjected to restriction digestion. The presence of TGT encoding the R155C VCP point mutation destroys an endogenous BtgI and a NciI restriction site in the human and murine VCP sequence, respectively, thus enabling the differentiation between wild-type and mutant mRNA species.

2.6. Data analysis and figure preparation

Data analysis was performed using Excel 2016 (Microsoft);

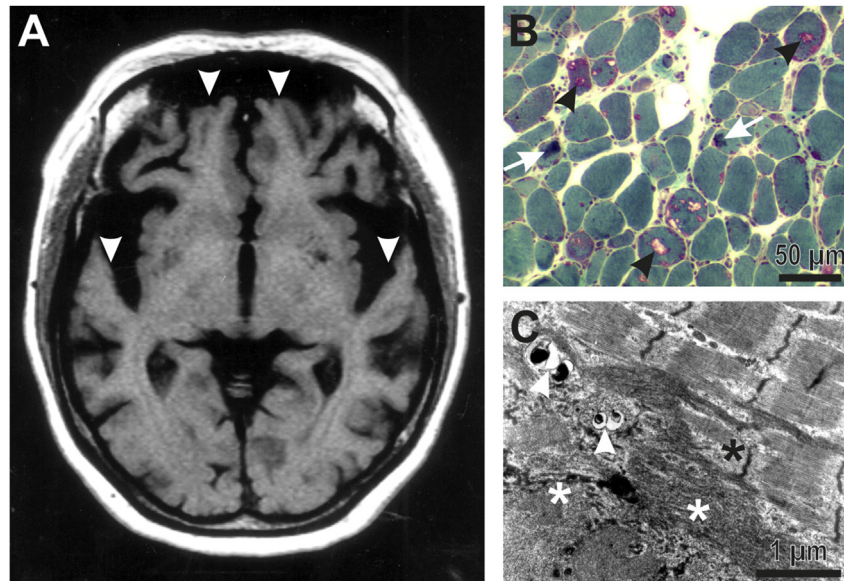


Fig. 2. Human R155C VCP related brain and skeletal muscle pathology. Cranial MRI and muscle pathology pictures are derived from a previously published IBMPFD patient with a heterozygous R155C VCP mutation [28]. **A**, T1-weighted cranial MRI illustrating the marked frontotemporal brain atrophy (white arrowheads). **B**, Gömöri trichrome stained skeletal muscle tissue specimen. Black arrowheads denote the presence of multiple rimmed vacuoles. White arrows indicate the presence of sarcoplasmic protein aggregates. **C**, Ultrastructural analysis of the same muscle specimen illustrating myofibrillar degeneration (black asterisk), autophagic vacuoles (white arrowheads), and sarcoplasmic protein aggregates (white asterisks). (For interpretation of the references to colour in this figure legend, the reader is referred to the Web version of this article.)

additional information is provided in the figure legends. Data of the phenotypic screen were analyzed by Student's t-test or linear model, as appropriate. Final assembly and preparation of all figures for publication was done using Corel Draw Graphics Suite X7.

3. Results

3.1. R155C VCP knock-in mice: a genetic model for human VCP-related diseases

To generate a R155C VCP knock-in mouse model, we used a gene targeting strategy that replaced the triplet “CGG” (human “CGT”) encoding arginine by “TGT” (human “TGT”) encoding cysteine in exon 5. As previously reported, our first approach did not lead to the generation of R155C VCP knock-in mice, but resulted in a mouse strain that was haploinsufficient for wild-type VCP (B6J.129S2-Vcp^{tm1.1Ccrs}, <http://www.informatics.jax.org/allele/MGI:6189547>; synonym: B6J.129S2-Vcp^{tm1(ko)CscI&RfSr}, supplementary figure 1 in Ref. [35]). Our second, modified gene targeting approach, in which we changed the position of the single remaining loxP site after Cre recombination to a more upstream location within intron 4 (Fig. 1B), finally led to the generation of the intended R155C VCP knock-in mice (B6J.B6-Vcp^{tm2.1Ccrs}, <http://www.informatics.jax.org/allele/MGI:6189550>). The correct targeting event was confirmed by PCR genotyping in conjunction with sequencing as well as Southern blotting (Fig. 1C and D). The presence of the mutant mRNA species coding for R155C VCP in ear tissue from the very first mice of this newly generated mouse strain was confirmed by RT-PCR and sequencing of the PCR products (Fig. 1E). Breeding of heterozygous R155C VCP knock-in mice did not yield in the generation of viable mice homozygous for the R155C VCP mutation. Notably, homozygosity could only be detected in tissue specimens from body parts of dead newborn mice. The latter finding indicates that the sole expression of R155C point mutant VCP exerts a deleterious effect not compatible with life.

3.2. From human IBMPFD pathology to comprehensive phenotyping of R155C VCP knock-in mice

The typical morphological correlate of a clinically manifest fronto-temporal dementia in humans is the prominent brain atrophy in the corresponding regions (Fig. 2A), whereas the typical myopathological picture of diseased skeletal muscle tissue comprises myopathic alterations in conjunction with an abundance of rimmed vacuoles, sarcoplasmic protein aggregates, and degenerating myofibrils (Fig. 2B and C). The primary question of this study was whether our newly generated heterozygous R155C VCP knock-in mouse strain may serve as an animal model that truly mirrors the human VCP-related pathology. However, our first phenotypic and histopathological analyses of skeletal muscle tissue from heterozygous R155C VCP knock-in mice did not provide any evidence of pathology. In order to look for a late-onset VCP-related pathology, we further performed a detailed myopathological analysis of aged, 16-month-old heterozygous R155C VCP knock-in mice which again showed no significant pathology. Moreover, our immunoblot analyses addressing the protein expression levels of the direct VCP interaction partner strumpellin (WASH complex subunit 5), key markers of autophagy (sequestosome-1/p62, BAG-3, Serine/threonine-protein kinase ULK1, Beclin-1), and TDP-43 as well as our proteasome activity measurements in skeletal muscle tissue of heterozygous R155C VCP knock-in mice displayed levels which were in the same range as in wild-type siblings (Fig. 3, “biochemistry” part). Subsequently we performed a very detailed and comprehensive phenotyping analysis in collaboration with the German Mouse Clinic. These analyses comprised a broad range of parameters including such related to neurology, behavior, dysmorphology, cardiovascular system, and general organ pathology. Again, this comprehensive screening did not reveal any pathology related to the human phenotypes of IBMPFD, ALS, or HSP. Notably, statistically significant alterations were observed in several tests related to clinical chemistry (decreased concentrations of plasma lactate, serum albumin and total protein), energy metabolism (increased oxygen consumption), hematology (decreased number

screen	method/parameter	phenotype (het R155C VCP KI vs. wild-type)
allergy	Ig-ELISA	no significant/marked difference
	transepidermal water loss	no significant/marked difference
behaviour	open field	no significant/marked difference
	acoustic startle & prepulse inhibition	no significant/marked difference
cardiovascular	electrocardiogram	no significant/marked difference
	echocardiography	no significant/marked difference
clinical chemistry	plasma lactate	9.4 vs. 10.4 mmol/l, p=0.002
	total protein	47.9 vs. 50.6 g/l, p=0.001
	albumin	27.2 vs. 29.5 g/l, p=0.0004
	other parameters from autoanalyzer	no significant/marked difference
	glucose tolerance test	no significant/marked difference
dysmorphology	visual inspection	no significant/marked difference
	X-ray	no significant/marked difference
	dual-energy X-ray absorptiometry	no significant/marked difference
energy metabolism	oxygen consumption (normalized to body mass)	76.3 vs. 73.4 ml O ₂ /h·animal, p<0.001
	other parameters from indirect calorimetry	no significant/marked difference
	qNMR	no significant/marked difference
eye	Scheimpflug imaging	no significant/marked difference
	optical coherence tomography	no significant/marked difference
	laser interference biometry	no significant/marked difference
	virtual drum	no significant/marked difference
hematology	platelets	712 vs. 880 10 ³ /mm ³ , p=0.006
	other blood counts	no significant/marked difference
immunology	CD8+/Ly6C+ T-cells	51.7 vs. 37.4%, p=0.0000005
	other parameters from flow cytometry	no significant/marked difference
	multiplex bead array	no significant/marked difference
neurology	modified SHIRPA	no significant/marked difference
	grip strength	no significant/marked difference
	rotarod	no significant/marked difference
	auditory brain stem response	no significant/marked difference
	nociception/hot plate	no significant/marked difference
pathology	macroscopy	44.4 vs. 52.1 mg liver/g body weight, p=0.0003
	histology (all organs/tissues)	no significant/marked difference
biochemistry	immunoblotting of VCP (p97), strumpellin, p62 (Sequestosome-1), BAG-3, TDP-43, ULK1, Beclin-1	identical protein expression levels
	chymotrypsin-like proteasome activity	no significant difference

Fig. 3. Comprehensive phenotypic analysis of heterozygous R155C VCP knock-in mice. A cohort of 6 female and 13 male heterozygous R155C VCP knock-in mice and 10 female and 11 male wild-type siblings were subjected to a comprehensive phenotyping at the German Mouse Clinic. Investigation started with mice aged 11 weeks and ended with age of 23 weeks. The conducted analyses and results of this standardized workflow are summarized in this simplified overview. Parameters that are significantly increased or decreased in heterozygous R155C VCP knock-in mice as compared to the wild-type controls are highlighted in green or orange, respectively, and the mean values with data of both sexes pooled are given. Statistical significance was calculated by Student's t-test or linear model, as appropriate. Further biochemical analyses addressing protein expression levels and proteasome function are given in a separate section (yellow). (For interpretation of the references to colour in this figure legend, the reader is referred to the Web version of this article.)

of platelets), immune system (increased percentage of Ly6C expressing CD8 T-cells), and organ pathology (decreased liver to body weight ratio) (Fig. 3). All results of the phenotypic screen are in detail available online in the German Mouse Clinic phenomap (www.mouseclinic.de).

3.3. VCP mRNA and protein expression in mice and men

Though our wide-range phenotypic analyses depicted several statistically significant abnormalities in our R155C VCP knock-in mice, none of them showed a direct or indirect relationship to the previously reported mutant VCP-related phenotypes in humans. This prompted us to study the VCP mRNA and protein levels in skeletal muscle in more detail. On the protein level, we detected no obvious differences in the total amount of VCP in normal and IBMPFD-derived human skeletal muscle carrying the R155C mutation as well as in skeletal muscle and brain tissue derived from wild-type and heterozygous R155C VCP knock-in mice (Fig. 4G). In a next step we determined the ratio of wild-type and mutant VCP mRNAs in the human skeletal muscle tissue by performing RT-PCRs in conjunction with BtgI restriction digestion (Fig. 4A). Further analysis and quantitation showed that 70% of total VCP mRNA is derived from the mutant allele (Fig. 4B). Notably, analogous experiments using skeletal muscle and brain tissue specimens from heterozygous R155C VCP knock-in mice only revealed the presence of 7% and 5% mutant VCP mRNA, respectively (Fig. 4C–F). To ascertain that this rather puzzling result is not influenced by sequence alterations affecting the NciI restriction digestion, we further sequenced and verified 12 colony PCR products derived from skeletal muscle and brain tissue from wild-type and heterozygous R155C VCP knock-in mice.

4. Discussion

The vital role of wild-type VCP protein is highlighted by several studies showing that the targeted ablation of VCP in *Trypanosoma brucei* [36], *Saccharomyces cerevisiae* [37], *Drosophila melanogaster* [38], and mouse [39] is lethal in all these organisms. In order to study the pathological consequences of mutant VCP expression, we here generated a R155C VCP knock-in mouse strain as a genetic model for the human IBMPFD disease. The codon 155 is a VCP mutation hot spot, and several different IBMPFD-causing missense mutations resulting in an amino acid substitution from arginine to cysteine (p.R155C [3,40]), to histidine (p.R155H [3]), to leucine (p.R155L [41]), to proline (p.R155P [3]), to serine (p.R155S [42]), and to glutamine (R155Q [43]) have been described. While our gene targeting approach yielded in the generation of the intended heterozygous R155C VCP knock-in mice, the failure to generate homozygous offspring clearly denotes a deleterious effect of the homozygous R155C mutation, which is not compatible with life. Our extensive analyses of the heterozygous R155C VCP knock-in mice revealed several statistically significant aberrations comprising decreased concentrations of plasma lactate, albumin, total protein, a decreased number of platelets, decreased liver to body weight ratio, an increased percentage of Ly6C expressing CD8 T-cells, and increased oxygen consumption. However, none of these wide-spread aberrations have previously been reported in the context of human VCP-related diseases. On the other hand, our R155C VCP knock-in mice did not show any clinical or morphological evidence suggesting the manifestation of IBMPFD, ALS, PD, HSP, or HMSN2.

Our findings in the R155C VCP knock-in mouse strain are in clear contrast to the previously published R155H VCP knock-in mouse strain. Heterozygous mice of this line were reported to display IBMPFD-related skeletal muscle, bone, and brain pathology [23] as

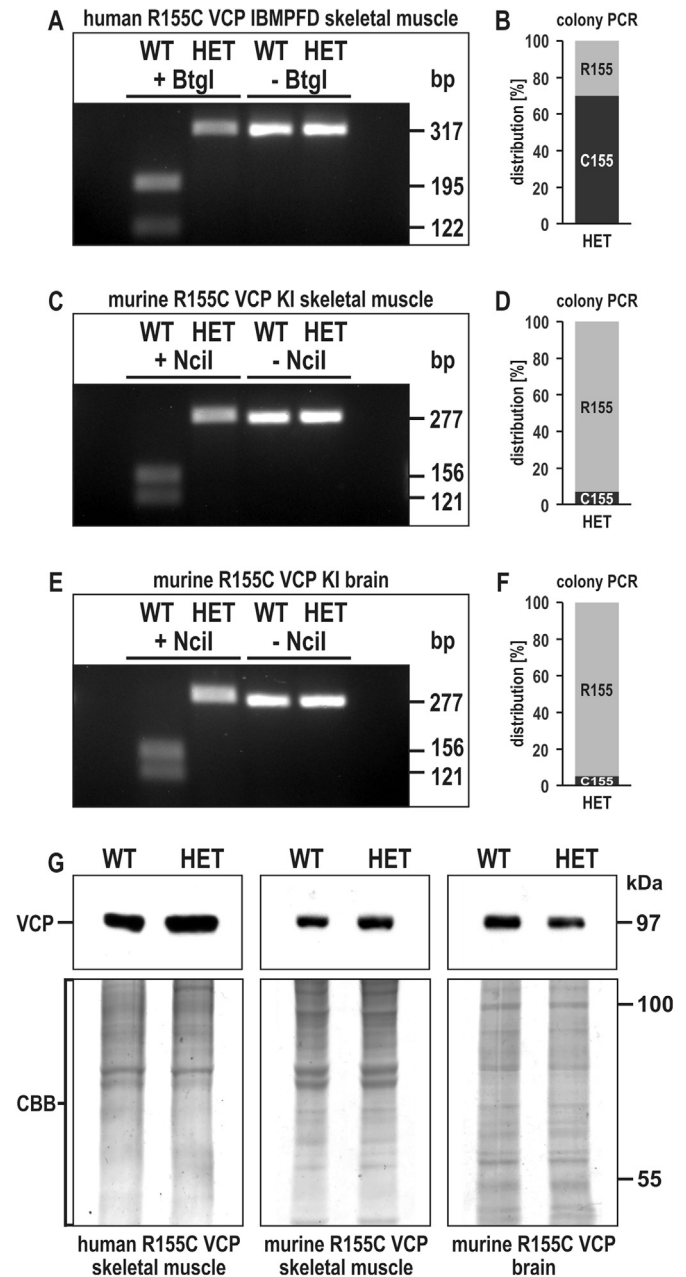


Fig. 4. Expression levels of wild-type and mutant VCP mRNA and protein in human and murine skeletal muscle as well as murine brain tissue. **A**, Wild-type and TGT, encoding R155C VCP mRNA expression analysis in human skeletal muscle tissue derived from a control (WT) and an IBMPFD patient (HET) by RT-PCR in conjunction with cloning of the PCR product, colony PCRs, and BtgI restriction digestion. Since the presence of the R155C mutation destroys an endogenous BtgI restriction digestion site, the 317 bp RT-PCR product derived from the mutant mRNA cannot be digested into the 195 and 122 bp fragments as seen in the normal control. **B**, Quantitation of the levels of wild-type (R155) and mutant (C155) VCP mRNA. BtgI restriction digestion of the PCR products from 124 single colonies identified 37 wild-type and 87 mutant VCP clones. The stacked column denotes the relative amounts in percent of the wild-type and mutant VCP mRNA species in the heterozygous R155C VCP patient. **C–F**, Analogous experiments were performed with skeletal muscle (107 single colonies; 99 wild-type and 8 mutant VCP clones) and brain (113 single colonies; 107 wild-type and 6 mutant VCP clones) tissue derived from R155C VCP knock-in mice. Here, the presence of the R155C mutation destroys an NciI restriction site. Note that the relative amounts of the mutant VCP mRNA species in skeletal muscle and brain tissue from heterozygous mice are far below the range observed in the human IBMPFD skeletal muscle tissue. **G**, Upper panel, VCP immunoblotting using total protein extracts from human and murine skeletal muscle as well as murine brain tissue. Note, that there is no significant difference in the VCP protein levels between the respective wild-type and heterozygous R155C VCP tissue samples. Lower panel, Coomassie brilliant blue stained SDS-PAGE gel as loading control.

well as ALS resembling spinal cord alterations with age-dependent degeneration of ventral horn motoneurons [44]. Though the R155H mutant VCP already evoked human IBMPFD-related pathologies in heterozygous mice, their mating also resulted in the successful generation of homozygous R155H VCP knock-in mice, which were reported to display an accelerated disease phenotype inevitably leading to premature death in the first three weeks after birth [45]. The findings in the R155H VCP knock-in mouse strain are further mirrored in two transgenic mouse strains overexpressing either the R155H or the A232E VCP mutant, which both display the aforementioned signs of IBMPFD pathology [46].

To address the striking clinical and pathomorphological differences between the R155H and our newly generated R155C VCP knock-in mouse strains, we performed analyses focusing on the VCP protein and mRNA levels in human IBMPFD and murine R155C VCP knock-in mice tissues specimens. In keeping with our previous immunoblot studies on human R155C, R155H, and R93C IBMPFD skeletal muscle specimens [28], our current analysis showed identical VCP protein levels in human IBMPFD tissue as compared to normal controls. This finding is also mirrored in skeletal muscle and brain tissue VCP immunoblots in both our R155C (Fig. 4G) and the R155H [23] VCP knock-in mouse strains. Thus, these results clearly show that different VCP missense mutations do not change the total endogenous VCP protein level. However, our experiments revealed a different picture at the mRNA level. Here, we found that in human R155C VCP IBMPFD skeletal muscle tissue a fraction of 70% of the total VCP mRNA is derived from the mutant allele. In contrast, in skeletal muscle and brain tissue derived from our R155C VCP knock-in mice we detected only 7 and 5%, respectively, of the R155C mutant VCP mRNA. Hence, the lack of an obvious IBMPFD/ALS phenotype in our heterozygous R155C VCP knock-in mice is likely due to this low level of mutant VCP mRNA. The concept of a critical threshold of mutant VCP for disease pathology is further substantiated by a previous study applying a tamoxifen-induced, Cre-mediated excision approach of the R155H VCP mutation in heterozygous knock-in mice. Here, a marked amelioration of the skeletal muscle pathology was reported as a consequence of a highly efficient (90%), Cre-mediated deletion of the exon 4 and the missense mutation-harboring exon 5 [47]. Thus, the aforementioned data in conjunction with our results support the notion that targeted therapeutic approaches that lower the level of mutant VCP mRNA can ameliorate the VCP-inflicted disease pathology.

The reason for the very low expression of the R155C VCP mutant mRNA in skeletal muscle and brain tissue of our knock-in mouse strain is currently unclear. We hypothesize that the presence of the missense mutation itself alters the biological half-life of the mutant VCP mRNA. In this line, the human R155C VCP mRNA would exhibit a much more prolonged half-life than its murine counterpart. As an alternative explanation one has to consider the possibility that the remaining single loxP site in intron 4 hampers the transcription rate, splicing machinery, or nuclear export. However, since the gene targeting approach for generation of the R155C as well as the R155H VCP knock-in mice strains both resulted in a loxP positioning in intron 4, the latter explanation seems to be rather unlikely.

Conflicts of interest

The authors declare that they have no conflict of interest.

Acknowledgements

CSC, LE, and RS were supported by the DFG within the framework of the multi-location research group FOR1228 (CL 381/3-1, CL 381/3-2, EI 399/5-1, EI 399/7-2, SCHR 562/9-1, SCHR 562/9-2). CSC

and RS were further supported by the Fritz Thyssen Foundation (grant 10.07.1.165). MT was supported by the Interdisciplinary Center for Clinical Research Erlangen. MHA was supported by the Infrafrontier grant 01KX1012.

CSC and RS jointly conceived the study, reviewed all data, prepared the figures, and wrote the manuscript. MHA conceived the phenotypic screen. HF and VGD the supervised phenotypic experiments. LW, KHS, LE, and CSC designed and carried out experiments and analyzed data. CB, MT, and CK carried out experiments and analyzed data. JAA, OVA, LB, LG, WH, KM, FN, LP, BR, IR, JR, and IT performed phenotypic experiments and analyzed data. AF carried out experiments. MV analyzed data. All authors read and approved the final version of manuscript text and figures. We thank Walter Witke, Institute of Genetics, University of Bonn, Germany, for critical reading of the manuscript.

Transparency document

Transparency document related to this article can be found online at <https://doi.org/10.1016/j.bbrc.2018.08.038>.

References

- [1] D. Halawani, M. Latterich, p97: the cell's molecular purgatory? *Mol. Cell* 22 (2006) 713–717.
- [2] L. Madsen, M. Seeger, C.A. Semple, et al., New ATPase regulators—p97 goes to the PUB, *Int. J. Biochem. Cell Biol.* 41 (2009) 2380–2388.
- [3] G.D. Watts, J. Wymer, M.J. Kovach, et al., Inclusion body myopathy associated with Paget disease of bone and frontotemporal dementia is caused by mutant valosin-containing protein, *Nat. Genet.* 36 (2004) 377–381.
- [4] R. Schröder, G.D. Watts, S.G. Mehta, et al., Mutant valosin-containing protein causes a novel type of frontotemporal dementia, *Ann. Neurol.* 57 (2005) 457–461.
- [5] J.O. Johnson, J. Mandrioli, M. Benatar, et al., Exome sequencing reveals VCP mutations as a cause of familial ALS, *Neuron* 68 (2010) 857–864.
- [6] N. Chan, C. Le, P. Shieh, et al., Valosin-containing protein mutation and Parkinson's disease, *Park. Relat. Disord.* 18 (2012) 107–109.
- [7] M. Regensburger, M. Türk, A. Pagenstecher, et al., VCP-related multisystem proteinopathy presenting as early-onset Parkinson disease, *Neurology* 89 (2017) 746–748.
- [8] S.T. de Bot, H.J. Schelhaas, E.J. Kamsteeg, et al., Hereditary spastic paraplegia caused by a mutation in the VCP gene, *Brain* 135 (2012), e223.
- [9] C.S. Clemen, L. Eichinger, R. Schröder, VCP: a jack of all trades in neuro- and myodegeneration? – Reply to the Letter to the Editor "Hereditary Spastic Paraplegia caused by a mutation in the VCP gene, *Brain* 135 (2012), e224.
- [10] M.A. Gonzalez, S.M. Feely, F. Spezziani, et al., A novel mutation in VCP causes Charcot-Marie-Tooth Type 2 disease, *Brain* 137 (2014) 2897–2902.
- [11] T. Evangelista, C.C. Weihl, V. Kimonis, et al., 215th ENMC international workshop VCP-related multi-system proteinopathy (IBMPFD) 13–15 November 2015, Heemskerk, The Netherlands, *Neuromuscul. Disord.* 26 (2016) 535–547.
- [12] B. DeLaBarre, A.T. Brunger, Complete structure of p97/valosin-containing protein reveals communication between nucleotide domains, *Nat. Struct. Biol.* 10 (2003) 856–863.
- [13] T.F. Chou, S.L. Bulfer, C.C. Weihl, et al., Specific inhibition of p97/VCP ATPase and kinetic analysis demonstrate interaction between D1 and D2 ATPase domains, *J. Mol. Biol.* 426 (2014) 2886–2899.
- [14] I. Rouiller, B. DeLaBarre, A.P. May, et al., Conformational changes of the multifunction p97 AAA ATPase during its ATPase cycle, *Nat. Struct. Biol.* 9 (2002) 950–957.
- [15] X. Zhang, A. Shaw, P.A. Bates, et al., Structure of the AAA ATPase p97, *Mol. Cell* 6 (2000) 1473–1484.
- [16] F. Beuron, I. Dreveny, X. Yuan, et al., Conformational changes in the AAA ATPase p97-p47 adaptor complex, *EMBO J.* 25 (2006) 1967–1976.
- [17] G.H. Baek, H. Cheng, V. Choe, et al., Cdc48: a Swiss army knife of cell biology, *J. Amino Acids* 2013 (2013) 183421.
- [18] H. Meyer, C.C. Weihl, The VCP/p97 system at a glance: connecting cellular function to disease pathogenesis, *J. Cell Sci.* 127 (2014) 3877–3883.
- [19] R. Rijal, K. Arhzaouy, K.H. Strucksberg, et al., Mutant p97 exhibits species-specific changes of its ATPase activity and compromises the UBXD9-mediated monomerisation of p97 hexamers, *Eur. J. Cell Biol.* 95 (2016) 195–207.
- [20] D. Ritz, M. Vuk, P. Kirchner, et al., Endolysosomal sorting of ubiquitylated caveolin-1 is regulated by VCP and UBXD1 and impaired by VCP disease mutations, *Nat. Cell Biol.* 13 (2011) 1116–1123.
- [21] Y. Erzurumlu, F.A. Kose, O. Gozen, et al., A unique IBMPFD-related P97/VCP mutation with differential binding pattern and subcellular localization, *Int. J. Biochem. Cell Biol.* 45 (2013) 773–782.

- [22] D. Barthelme, R. Jauregui, R.T. Sauer, An ALS disease mutation in Cdc48/p97 impairs 20S proteasome binding and proteolytic communication, *Protein Sci.* 24 (2015) 1521–1527.
- [23] M. Badadani, A. Nalbandian, G.D. Watts, et al., VCP associated inclusion body myopathy and paget disease of bone knock-in mouse model exhibits tissue pathology typical of human disease, *PLoS One* 5 (2010).
- [24] V. Gailus-Durner, H. Fuchs, L. Becker, et al., Introducing the German Mouse Clinic: open access platform for standardized phenotyping, *Nat. Methods* 2 (2005) 403–404.
- [25] H. Fuchs, V. Gailus-Durner, T. Adler, et al., The German Mouse Clinic: a platform for systemic phenotype analysis of mouse models, *Curr. Pharmaceut. Biotechnol.* 10 (2009) 236–243.
- [26] H. Fuchs, V. Gailus-Durner, S. Neschen, et al., Innovations in phenotyping of mouse models in the German Mouse Clinic, *Mamm. Genome* 23 (2012) 611–622.
- [27] H. Fuchs, V. Gailus-Durner, T. Adler, et al., Mouse phenotyping, *Methods* 53 (2011) 120–135.
- [28] C.U. Hübbbers, C.S. Clemen, K. Kesper, et al., Pathological consequences of VCP mutations on human striated muscle, *Brain* 130 (2007) 381–393.
- [29] V. Dubowitz, C. Sewry, A. Oldfors, *Muscle Biopsy: a Practical Approach*, fourth ed., Saunders/Elsevier Ltd., Oxford, 2013.
- [30] L. Winter, I. Wittig, V. Peeva, et al., Mutant desmin substantially perturbs mitochondrial morphology, function and maintenance in skeletal muscle tissue, *Acta Neuropathol.* 132 (2016) 453–473.
- [31] L. Winter, I. Staszewska, E. Mihailovska, et al., Chemical chaperone ameliorates pathological protein aggregation in plectin-deficient muscle, *J. Clin. Invest.* 124 (2014) 1144–1157.
- [32] C.S. Clemen, F. Stöckigt, K.H. Strucksberg, et al., The toxic effect of R350P mutant desmin in striated muscle of man and mouse, *Acta Neuropathol.* 129 (2015) 297–315.
- [33] A. Chopard, F. Pons, P. Charpiot, et al., Quantitative analysis of relative protein contents by Western blotting: comparison of three members of the dystrophin-glycoprotein complex in slow and fast rat skeletal muscle, *Electrophoresis* 21 (2000) 517–522.
- [34] K.H. Strucksberg, K. Tangavelou, R. Schröder, et al., Proteasomal activity in skeletal muscle: a matter of assay design, muscle type, and age, *Anal. Biochem.* 399 (2010) 225–229.
- [35] C.S. Clemen, M. Marko, K.H. Strucksberg, et al., VCP and PSMF1: antagonistic regulators of proteasome activity, *Biochem. Biophys. Res. Commun.* 463 (2015) 1210–1217.
- [36] J.R. Lamb, V. Fu, E. Wirtz, et al., Functional analysis of the trypanosomal AAA protein TbVCP with trans-dominant ATP hydrolysis mutants, *J. Biol. Chem.* 276 (2001) 21512–21520.
- [37] K.U. Fröhlich, H.W. Fries, M. Rudiger, et al., Yeast cell cycle protein CDC48p shows full-length homology to the mammalian protein VCP and is a member of a protein family involved in secretion, peroxisome formation, and gene expression, *J. Cell Biol.* 114 (1991) 443–453.
- [38] A. Leon, D. McKearin, Identification of TER94, an AAA ATPase protein, as a Bam-dependent component of the *Drosophila* fusome, *Mol. Biol. Cell* 10 (1999) 3825–3834.
- [39] J.M. Müller, K. Deinhardt, I. Rosewell, et al., Targeted deletion of p97 (VCP/CDC48) in mouse results in early embryonic lethality, *Biochem. Biophys. Res. Commun.* 354 (2007) 459–465.
- [40] P. Gonzalez-Perez, E.T. Cirulli, V.E. Drory, et al., Novel mutation in VCP gene causes atypical amyotrophic lateral sclerosis, *Neurology* 79 (2012) 2201–2208.
- [41] K.R. Kumar, M. Needham, K. Mina, et al., Two Australian families with inclusion-body myopathy, Paget's disease of bone and frontotemporal dementia: novel clinical and genetic findings, *Neuromuscul. Disord.* 20 (2010) 330–334.
- [42] T. Stojkovic, H. Hammouda el, P. Richard, et al., Clinical outcome in 19 French and Spanish patients with valosin-containing protein myopathy associated with Paget's disease of bone and frontotemporal dementia, *Neuromuscul. Disord.* 19 (2009) 316–323.
- [43] V.E. Kimonis, S.G. Mehta, E.C. Fulchiero, et al., Clinical studies in familial VCP myopathy associated with Paget disease of bone and frontotemporal dementia, *Am. J. Med. Genet. A* 146A (2008) 745–757.
- [44] H.Z. Yin, A. Nalbandian, C.I. Hsu, et al., Slow development of ALS-like spinal cord pathology in mutant valosin-containing protein gene knock-in mice, *Cell Death Dis.* 3 (2012) e374.
- [45] A. Nalbandian, K.J. Llewellyn, M. Kitazawa, et al., The homozygote VCP^(R155H/R155H) mouse model exhibits accelerated human VCP-associated disease pathology, *PLoS One* 7 (2012), e46308.
- [46] S.K. Custer, M. Neumann, H. Lu, et al., Transgenic mice expressing mutant forms VCP/p97 recapitulate the full spectrum of IBMPFD including degeneration in muscle, brain and bone, *Hum. Mol. Genet.* 19 (2010) 1741–1755.
- [47] A. Nalbandian, K.J. Llewellyn, C. Nguyen, et al., Targeted excision of VCP R155H mutation by Cre-LoxP technology as a promising therapeutic strategy for valosin-containing protein disease, *Hum. Gene Ther. Meth.* 26 (2015) 13–24.